



# Electrochemical reduction of CO<sub>2</sub> over Sn-Nafion<sup>®</sup> coated electrode for a fuel-cell-like device

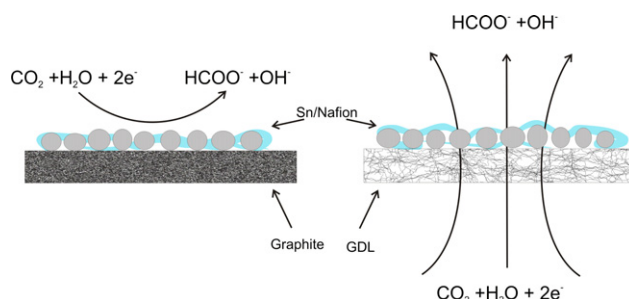
G.K. Surya Prakash\*, Federico A. Viva<sup>1</sup>, George A. Olah

Loker Hydrocarbon Research Institute and Department of Chemistry, University of Southern California, Los Angeles, CA 90089, USA

## HIGHLIGHTS

- ▶ Commercially available Sn particles for electrochemical reduction of CO<sub>2</sub> to formate.
- ▶ Measurements of electrocatalytic activity of metallic Sn and Sn powder catalysts.
- ▶ CO<sub>2</sub> reduction potentiostatically in sodium bicarbonate solution at ambient CO<sub>2</sub> pressure.
- ▶ The exchange current density of Sn gas diffusion electrode is two orders of magnitude higher over metallic Sn disc.
- ▶ Current density of 27 mA cm<sup>-2</sup> (−1.6 V per NHE) at 70% faradaic efficiency towards HCOO<sup>−</sup> formation.

## GRAPHICAL ABSTRACT



## ARTICLE INFO

### Article history:

Received 22 June 2012

Received in revised form

7 September 2012

Accepted 8 September 2012

Available online 20 September 2012

### Keywords:

Electrochemical reduction

CO<sub>2</sub>

Sn

Formic acid

Fuel cell-like device

## ABSTRACT

Commercially available Sn particles mixed with Nafion<sup>®</sup> ionomer are used to prepare an electrode with a gas diffusion layer support in a manner similar to that in which fuel cell electrodes are prepared. Cyclic voltammetry is performed in aqueous NaHCO<sub>3</sub> (basic medium) on the electrode and the Tafel parameters are obtained and compared with a Sn metal disc and with a graphite disc coated with Sn powder. In addition, electrolysis is carried out potentiostatically, also in NaHCO<sub>3</sub> solution, at various potentials. The exchange current density on the Sn/gas diffusion layer electrode shows to be two orders of magnitude higher than that on the metallic Sn disc. The maximum current density obtained during electrolysis is 27 mA cm<sup>-2</sup> at −1.6 V vs. NHE, with 70% faradaic efficiency towards the formation of formate, which is one of the highest values found in the literature on Sn electrode at ambient pressure.

© 2012 Elsevier B.V. All rights reserved.

## 1. Introduction

The chemical or electrochemical reduction of carbon dioxide has been envisioned as a possible answer to address global challenges, such as the depletion of fossil fuels, which are non-renewable on the human timescale and the reduction of man made emission of carbon dioxide, which is tied to global climate change [1–5].

\* Corresponding author. Tel.: +1 213 740 5984; fax: +1 213 740 6679.

E-mail address: [gprakash@usc.edu](mailto:gprakash@usc.edu) (G.K.S. Prakash).

<sup>1</sup> Present address: Grupo Celdas de Combustible, Departamento de Física de la Materia Condensada, Centro Atómico Constituyentes, Comisión Nacional de Energía Atómica (CNEA), Av General Paz 1499 (1650), San Martín, Buenos Aires, Argentina.

Converting CO<sub>2</sub> into simple molecules such as methanol and dimethyl ether, which are useful fuels and feed-stocks, on a large scale will address these problems [3,6]. These molecules can subsequently be transformed into more complex products such as ethylene and/or propylene, the major feed-stocks of the petrochemical industry, currently derived from oil and gas [1,4,5]. The ideal carbon source should ultimately be atmospheric carbon dioxide [1,4,5,7] to counteract the climate change caused by increasing anthropogenic emissions. In other words, CO<sub>2</sub> reduction is an energy storage strategy: electrical energy from any carbon neutral source—such as hydroelectric, solar, wind, geothermal, tidal, or nuclear—can be stored as chemical energy in the resulting products of reduction. This is particularly important for intermittent power sources, like solar, wind and tidal waves in which power generation does not match power demand. For example, photovoltaic solar plants produce no power when there is no sun. Excess power from these sources can be used to reduce CO<sub>2</sub> to gaseous or liquid fuels, which are portable and can be stored and used as needed in fuel cell devices. Consumption of these fuels produces carbon dioxide, closing the cycle. Sequestration and storage is commonly proposed as a method for decreasing atmospheric CO<sub>2</sub> [1]. However, we believe that the reduction of carbon dioxide to useful feed-stocks and energy carriers would be a more permanent solution. In this context, carbon dioxide can be conveniently captured at point sources such as fossil fuel burning power plants, aluminium plants, fermentation units and cement plants [8,9]. Electrochemical reduction of CO<sub>2</sub> gives way to a number of products containing one or two carbon atoms depending on the electrode material, nature of the solvent, local pH, electrolyte and CO<sub>2</sub> pressure [2,10–33]. In aqueous media, formic acid is produced with high selectivity and high faradaic efficiency (*f*) on In, Pb and Sn in HCO<sub>3</sub><sup>−</sup> electrolyte [18,24,32,34–41]. Formic acid is a good candidate as a fuel for fuel cells [42–44] and recently has been proposed as an optimal hydrogen carrier [45,46]. There is still some controversy regarding the mechanism of CO<sub>2</sub> reduction to formic acid, and particularly the nature of the reacting species. Ever since Paik et al. [47] first proposed a mechanism, it has generally been accepted that on the aforementioned metals (i.e. those with a high hydrogen overvoltage and a low affinity for CO adsorption), the radical anion CO<sub>2</sub><sup>•−</sup> receives a proton from a proton donor (water) and an electron to produce the formate ion. The pH of the bicarbonate electrolyte favours the dissolution of CO<sub>2</sub>, but the equilibrium reduces the number of hydronium ions in solution. Recently, Narayanan et al. described electrochemical conversion of CO<sub>2</sub> using Nafion based alkaline membrane electrodes employing indium and lead electrodes to produce formate in good faradaic efficiencies [48]. Previously, Mahammod et al. have reported the use of gas diffusion electrodes for high rate electrochemical reduction of CO<sub>2</sub> on lead, indium and tin under acidic conditions (pH ~2) [49].

In the present work, the electrochemical reduction of CO<sub>2</sub> was assessed by cyclic voltammetry on a gas diffusion layer (GDL) electrode, with Sn particles (SnGDL) applied in the form of a Nafion<sup>®</sup> ionomer ink, in a gas flow electrochemical cell. Tafel parameters were obtained from the voltammograms. The same determinations were performed on a flat Sn electrode (SnB), as well as a graphite disc electrode painted with the same Sn-Nafion<sup>®</sup> ink (SnG) for comparison. Sn was chosen from among the metals with high faradaic efficiency for formate because of its low cost and relatively low toxicity. In addition, electrolysis was performed potentiostatically on the GDL electrode to quantify the current density and the faradaic efficiency (*f*). In this study, a tin catalyst-coated gas diffusion layer in a membrane electrode assembly has been studied for suitability as the cathode for the electrochemical reduction of CO<sub>2</sub> and its performance evaluated when it was used in a fuel cell-like device as illustrated in Fig. 1

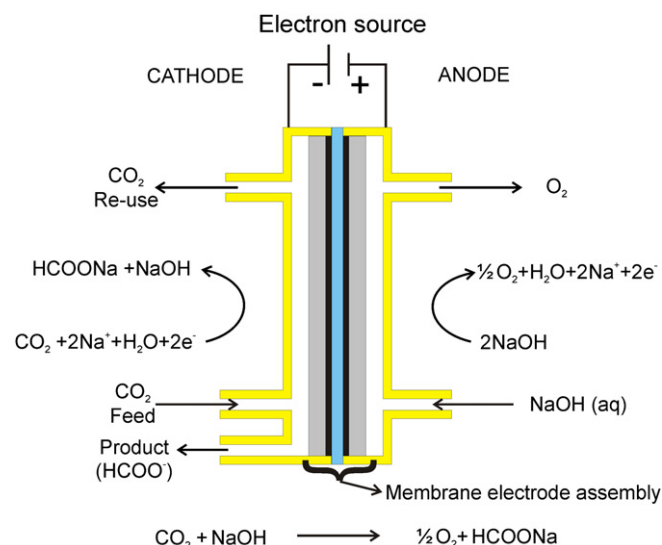


Fig. 1. Schematic representation of the CO<sub>2</sub> electroreduction in a fuel cell-like type of device.

## 2. Experimental

Cyclic voltammetry was performed on three different working electrodes (WE): a Sn metal disc (99.9%, Alfa Aesar); Sn powder (−100 mesh, 99.5%, Alfa Aesar) bonded to a graphite disc (99%, Aldrich) with Nafion<sup>®</sup> ionomer (5% in LW alcohols, Aldrich); and Sn powder, also bonded with Nafion<sup>®</sup> ionomer to a GDL (Toray carbon paper, TGP-H-60), i.e. a gas diffusion electrode (GDE). The geometric electrode areas of the Sn disc and the graphite disc were each 1 cm<sup>2</sup> while the GDE had an area of 9 cm<sup>2</sup>. The Sn disc was polished with a 1 μm alumina suspension on a cloth prior to use. The Sn ink was prepared by weighing Sn powder, Nafion<sup>®</sup> ionomer and water in a 1:1:1 proportion, and spread over the graphite disc and the GDL. The final Sn weight on the electrode was 6.8 mg cm<sup>−1</sup> over the graphite disc and 0.7 mg cm<sup>−1</sup> over the GDL. For the Sn disc electrode and the Sn-powder-coated graphite disc, a conventional three-compartment electrochemical cell was used. Meanwhile, for the GDE, a gas-flow cell was specially designed. Fig. 2 shows a schematic of this cell. In both cells, the counter electrode (CE) compartment was separated from the main compartment by a glass frit, while the reference electrode (RE) compartment was connected to the main compartment through a Luggin capillary. The reference electrode used in all measurements was a Ag/AgCl (ss) (Metrohm) and all the potentials reported were converted to the normal hydrogen electrode (NHE) scale (−0.197 V vs. Ag/AgCl). The counter electrode used was a coiled Pt wire (99.9%, 7.9 cm<sup>2</sup> area, Alfa Aesar). The electrolyte used was 0.5 M NaHCO<sub>3</sub> solution prepared from the solid salt (granular, ACS reagent, Aldrich) and milli-Q water (Direct-Q 3 system, Millipore), which had a pH ca. 8.3. Measurements were performed after degassing the solution for 30 min with either Ar (ultra high purity, Gilmore), used as a baseline, or CO<sub>2</sub> (99.998%, research grade, Gilmore) for the actual determinations. Cyclic voltammetry was performed with a Solartron SI 1287. Data fitting to obtain the Tafel parameters was performed with the Solartron instrument software. Geometrical areas were used to calculate current densities (*j*).

Electrolysis was performed potentiostatically between −0.8 and −2.0 V vs. NHE on the GDE prepared with Sn powder. CO<sub>2</sub> was sparged through the cell throughout the electrolysis at a flow rate of 4 mL min<sup>−1</sup>. The amount of formic acid, generated by the acidolysis of the sodium formate obtained by the reduction of carbon

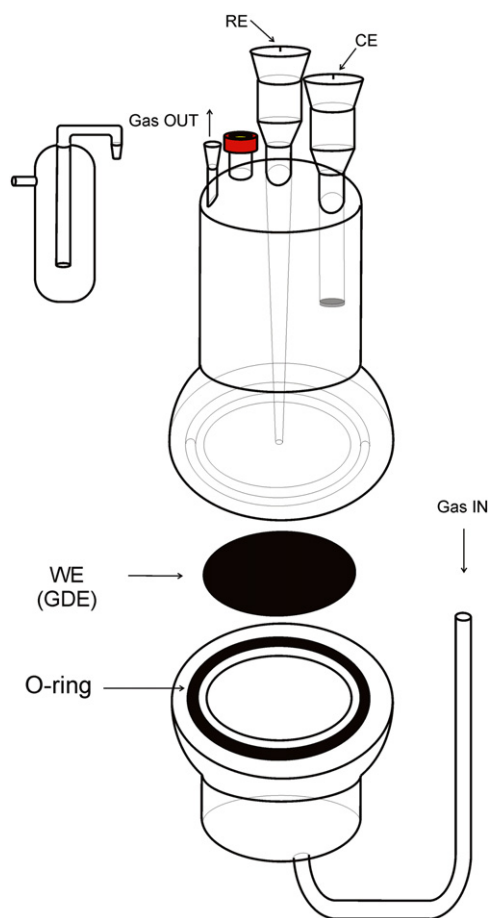


Fig. 2. Electrochemical cell used for the determination with Sn powder on a GDL.

dioxide, was quantified using a Thermo Finnigan Surveyor High Performance Liquid Chromatography (HPLC) system with an ultraviolet (UV) detector and using a SupelcoGel C-610H column to identify low-molecular weight carboxylic acids (30 cm × 7.8 mm, Supelco). Experiments were terminated when the total charge passed reached 200 C. Such a quantity of charge assured a measurable quantity of formate at every potential.

### 3. Results and discussion

#### 3.1. Voltammetric measurements

The cyclic voltammograms obtained for the three different kinds of electrodes are shown in Fig. 3. Fig. 3A depicts the voltammograms for the bulk Sn (SnB) metal disc electrode in 0.5 M NaHCO<sub>3</sub> solution degassed with argon gas (Ar) and saturated with CO<sub>2</sub>. The anodic peaks between −0.2 V and −0.5 V and the cathodic peak at ca. −1.1 V were reported by Kapusta et al. [50] and attributed to the formation and reduction of tin oxides in basic media. Zhou and coworkers [51], in voltammetric experiments carried out in NaHCO<sub>3</sub> by quartz crystal microbalance, have observed the absorption of carbonate species on the copper oxides formed at similar potentials. On the cathodic end of the voltammograms, an increase in the absolute current value can be observed in both cases. In the baseline, this increase is due to hydrogen evolution, while when the solution is saturated with CO<sub>2</sub> the enhanced current represents its reduction to formate. The onset potential for the CO<sub>2</sub> reduction reaction is 100 mV more anodic than the onset of

the H<sub>2</sub> evolution and the magnitude of the current for the former process is twice that of the latter. This shows that the reduction of CO<sub>2</sub> is more favourable than the evolution of H<sub>2</sub> on the Sn electrode.

The voltammograms for the Sn-powder-coated graphite disc (SnG) are shown in Fig. 3B, and those for the Sn-powder-decorated GDL (SnGDL) in Fig. 3C. The main features from Fig. 3A are still present, although the peaks mentioned above are broader due to the increased surface area. In particular, on the SnGDL, the shift of the anodic peaks to a more positive potential, in the presence of carbon dioxide, is more evident compared to the other two electrodes. The influence on the peak shift might be due to the CO<sub>2</sub> adsorption prior to the oxide formation or HCO<sub>3</sub><sup>−</sup> adsorption. In terms of the current arising from the reduction reaction, the onset potentials of the curves for the Sn powder electrodes move even further anodic than in the case of the SnB electrode relative to the voltammograms with Ar only. In the case of SnG, the shift is ca. 200–300 mV while for SnGDL it is more than 300 mV. At the same time, the current at the onset potential increases by three-to-four fold that of the Ar baseline on both SnG and SnGDL electrodes. The current density reached with the SnG is slightly higher than the one obtained with SnGDL, which is likely caused by the disruption of the reaction due to carbon dioxide flowing through the GDE. Still, the current density on the SnGDL is higher than that on the bulk metal electrode.

From the voltammograms, the corresponding Tafel plots for the three different electrodes were obtained and are shown in Fig. 4. The linear region of the plot obeys the Tafel equation [52], which relates the overpotential ( $\eta$ ) to the current density ( $j$ ). The linear fit of the plot yields the exchange current density ( $j_0$ ) from the current intercept while the slope ( $b$ ) contains the symmetry factor ( $\alpha$ ) commonly reported in mV decade<sup>−1</sup>. Parameters obtained from these plots are presented in Table 1. The SnB electrode is the only one that can be compared with the literature data, since Tafel plots and their parameters are typically reported for bulk metal electrodes. The equilibrium or rest potential ( $E_{eq}$ ) obtained for the Sn metal disc (Table 1) is close to the tabulated standard potential (−0.11 V vs. NHE) [53]. The values for the Tafel slopes are close in value to those published previously. Both Kapusta [54] and Vassiliev [32] reported a slope of ca. 120 mV decade<sup>−1</sup> for the region of lower overpotential, while for the high overpotential region, the reported value was 300–350 mV decade<sup>−1</sup>. The low overpotential region from this study agrees fairly well with the reported value, which corresponds to a symmetry factor of 0.5. In the high overpotential region (−0.9 to −0.3 V), the concomitant evolution of H<sub>2</sub> introduces some difficulty to the slope determination, and therefore the value obtained is somewhat higher but still on the same order as the reported value. The exchange current density obtained differs by three orders of magnitude from the one reported by Kapusta (10<sup>−9</sup> A cm<sup>−2</sup>) [54]. However, Vassiliev [32] showed that the electrolyte concentration and cation used may account for such a difference.

The values obtained for the other two types of electrodes differ from those of the bulk metal one, as expected for high surface area electrodes. The standard redox potentials determined from the experimental data are higher for both supported Sn powder electrodes, indicating that the reduction requires less energy for those electrode morphologies. Comparison of  $j_0$  between the bulk electrode and the ones prepared with the metal particles is pointless as the geometric area was used to calculate the current density. However, a comparison can be made between the two powder electrodes. In principle the real area per cm<sup>2</sup> of geometrical area for SnG and SnGDL should be almost the same. But the  $j_0$  value obtained on the SnGDL is five times higher than the one on the SnG electrode indicating a better utilization of the catalyst on the GDL support. Although the current density based on the geometrical

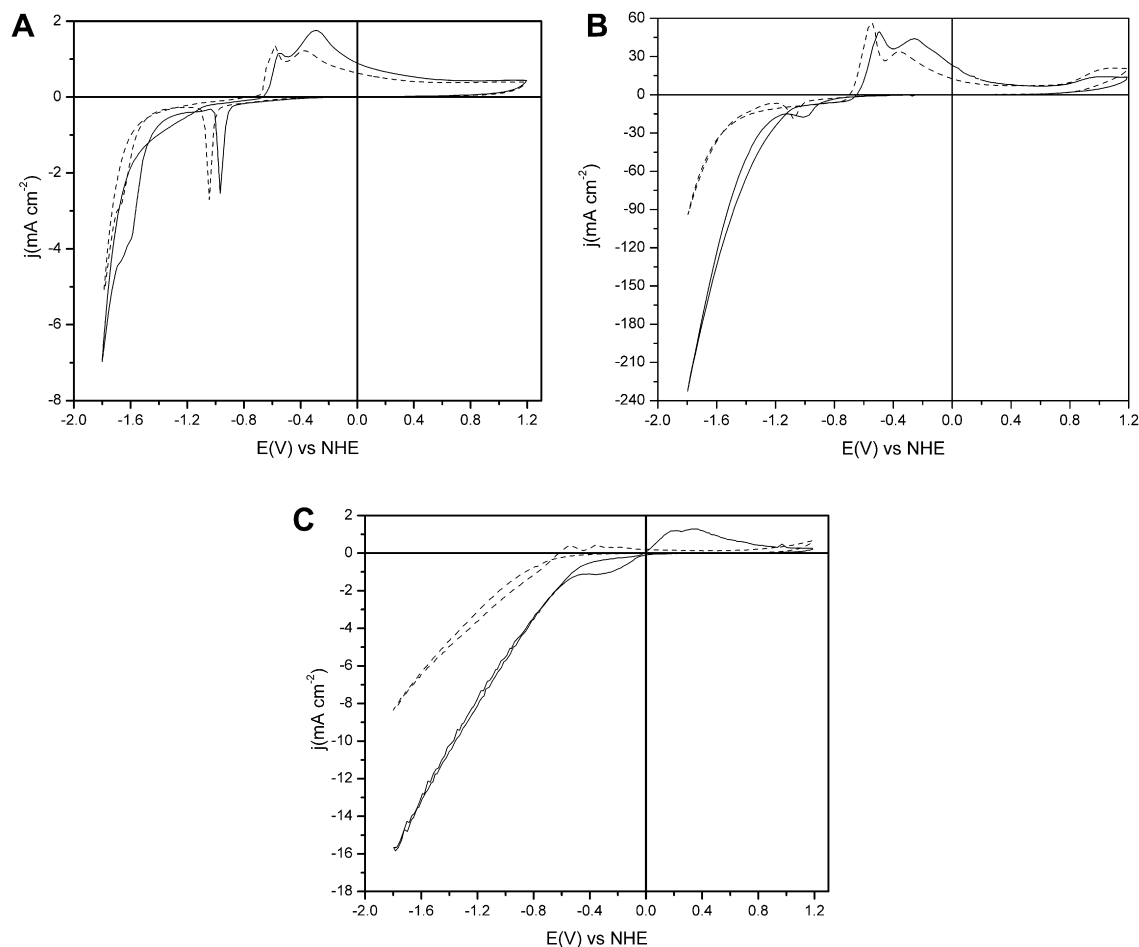


**Fig. 3.** A. Cyclic voltammograms in 0.5 M  $\text{NaHCO}_3$  on the SnB electrode at  $100 \text{ mV s}^{-1}$ . Degassed with Ar (dashed line). Saturated with  $\text{CO}_2$  (solid line). CV data labelling may need to be interchanged. B. Cyclic voltammograms in 0.5 M  $\text{NaHCO}_3$  on the SnG electrode at  $100 \text{ mV s}^{-1}$ . Degassed with Ar (dashed line). Saturated with  $\text{CO}_2$  (solid line). C. Cyclic voltammograms in 0.5 M  $\text{NaHCO}_3$  on the SnGDL electrode at  $100 \text{ mV s}^{-1}$ . Degassed with Ar (dashed line). Saturated with  $\text{CO}_2$  (solid line).

area was better for SnG than for SnGDL, the  $j_0$  supports the use of GDL as catalyst substrate. In terms of the Tafel slopes for SnG, the values are slightly higher in both regions compared to the bulk metal. Nevertheless, all values are consistent with each other and

with the bulk metal maintaining the same trend, therefore it can be concluded that there was no substantial change in the reduction mechanism. Overall, the values indicate a more facile reduction on the supported powder electrodes.

### 3.2. Electrochemical reduction of carbon dioxide

Electrolysis of carbon dioxide to obtain formic acid was performed on the SnGDL electrode. The electrolysis was performed potentiostatically at potentials between  $-0.8$  and  $-2.0 \text{ V}$  vs. NHE at  $0.2 \text{ V}$  intervals. The electrolyte used was the same as in the voltammetric experiments described in Section 3.1, and a low flow ( $4 \text{ mL min}^{-1}$ ) of carbon dioxide was maintained through the solution and over the electrode throughout the entire experiment. The reduction was performed potentiostatically because under a constant potential, the reaction current is determined by the

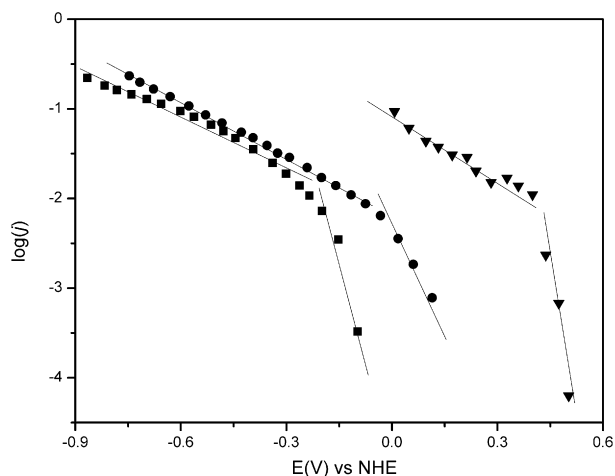


**Fig. 4.** Tafel plots obtained from the corresponding voltammograms. SnB (■), SnG (●) and SnGDL (▲).

**Table 1**

Tafel parameters obtained from the Tafel plots (Fig. 4).  $b_{c1}$  represents the slope for the lower overpotential region and  $b_{c2}$  for the high overpotential region.

	SnB	SnG	SnGDL
$b_{c1}$ (mV)	116	180	185
$b_{c2}$ (mV)	430	480	458
$j_0$ ( $\text{A cm}^{-2}$ )	$1.2 \times 10^{-6}$	$2.8 \times 10^{-5}$	$1.6 \times 10^{-4}$
$E_{eq}$ (V)	$-0.10$	0.030	0.053

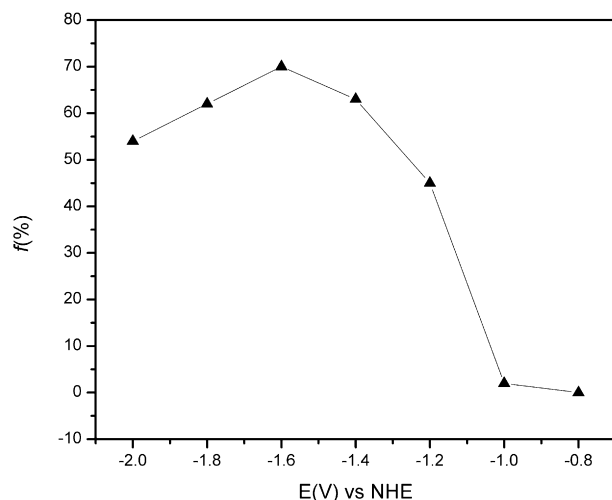


Fig. 5. Formic acid faradaic yields vs. potential for SnGDL.

system, showing how fast the reaction proceeds. Reduction current density was recorded at each potential, while the measured quantity of the formate was used to calculate the faradaic efficiency [52] based on the total charge passed through the cell.

Fig. 5 plots the faradaic efficiencies for formate obtained from the reduction of carbon dioxide versus the potential. Table 2 gives the corresponding values and the current densities for each experiment. Hydrogen was detected at every potential, and in a few cases (at  $-0.8$  V and  $-1.0$  V), carbon monoxide was detected in trace amounts as well. The trend shown in Fig. 5 for the faradaic efficiency versus the potential agrees with those reported in the literature for Sn metal electrodes [14,24,40,55–57]. Current density and faradaic efficiency increased as the potential decreased, reaching a maximum at  $-1.6$  V vs NHE, before decreasing at more negative potentials. At  $-1.6$  V a faradaic efficiency of 70% with a current density of  $27 \text{ mA cm}^{-2}$  was obtained. This faradaic efficiency is one of the highest found in the literature for Sn under basic conditions. Under low pH ( $\sim 2$ ), very high current densities on a GDL lead electrode have been reported (up to  $115 \text{ mA cm}^{-2}$ ) [49]. For electrolysis on bulk Sn metal performed under similar conditions, Noda et al. [57] reported a  $f$  of 63% with a  $j$  of  $3.8 \text{ mA cm}^{-2}$  at  $-1.4$  V vs. SHE. Koleli et al. [40] carried out the electrolysis on a fixed-bed reactor with Sn and Pb, and the best faradaic efficiency obtained on Sn was 74%, but with a current density below  $1.5 \text{ mA cm}^{-2}$ . Recently, a series of works were published with GDL-type electrodes [58–60]. Machunda and coworkers [59] also obtained 70% faradaic efficiency at  $-1.6$  V but with current densities below  $5 \text{ mA cm}^{-2}$ . Only Li et al. reported [58] comparable results: a faradaic efficiency of 86% with a current density of  $22 \text{ mA cm}^{-2}$ , and  $178 \text{ mA cm}^{-2}$  with a faradaic efficiency of 36%. Narayanan and

coworkers published [48] the only work so far about  $\text{CO}_2$  electro-reduction in a fuel cell like device with a GDL electrode under basic conditions. They used In and Pb as electrocatalysts and a Nafion membrane in alkaline media. It is proposed that the charge transfer is through  $\text{Na}^+$  ions similar as is presented in this work for experiments conducted in a three electrode cell. The work shows that the electrochemical reduction in a fuel cell type device is possible. The use of Sn metal particles bound with Nafion can be used in a similar device producing a significant amount of product (formate) with the advantage of using Sn, which is cheaper than In and less toxic than Pb.

#### 4. Conclusions

The results presented show that an electrode formed of Sn powder bound with Nafion® to a GDL gave high current densities and showed high efficiency for the reduction of carbon dioxide to formate under potentiostatic conditions. The exchange current density determined by Tafel plots from the cyclic voltammograms shows a fivefold increase on the SnGDL electrode compared to the SnG electrode, indicating a better catalyst utilization in the former. This improvement was demonstrated by the current density values obtained during electrolysis experiments. At  $-1.6$  V vs. NHE, a current density of  $27 \text{ mA cm}^{-2}$  was obtained with a faradaic efficiency of 70% for  $\text{CO}_2$  to formate reduction. It is expected that an electrolysis device using this catalyst will provide good results in terms of product formation.

#### Acknowledgements

Support of our work by the Department of Energy is gratefully acknowledged. FAV is a permanent research fellow of CONICET (Argentina).

#### References

- [1] G.A. Olah, A. Goeppert, G.K.S. Prakash, *Beyond Oil and Gas: The Methanol Economy*, second ed., John Wiley & Sons, Inc., Weinheim, 2009.
- [2] M. Gattrell, N. Gupta, A. Co, J. Electroanal. Chem. 594 (2006) 1–19.
- [3] F.R. Keene, in: B.P. Sullivan, K. Krist, H.E. Guard (Eds.), *Electrochemical and Electrocatalytic Reactions of Carbon Dioxide*, Elsevier, Amsterdam, 1993, pp. 1–16.
- [4] G.A. Olah, A. Goeppert, G.K.S. Prakash, J. Org. Chem. 74 (2009) 487–498.
- [5] G.A. Olah, G.K.S. Prakash, A. Goeppert, J. Am. Chem. Soc. 133 (2011) 12881–12898.
- [6] T. Weimer, K. Schaber, M. Specht, A. Bandi, Energy Convers. Manage. 37 (1996) 1351–1356.
- [7] A. Goeppert, M. Czaun, G.K.S. Prakash, G.A. Olah, Energy Environ. Sci. 5 (2012) 7833–7853.
- [8] A. Goeppert, S. Meth, G.K.S. Prakash, G.A. Olah, Energy Environ. Sci. 3 (2010) 1949–1960.
- [9] A. Goeppert, M. Czaun, R. May, G.K.S. Prakash, G.A. Olah, S. Narayan, J. Am. Chem. Soc. 133 (2011) 20164–20167.
- [10] C. Amatore, L. Nadjo, J.M. Saveant, New J. Chem. 8 (1984) 565–566.
- [11] C. Amatore, J.M. Saveant, J. Am. Chem. Soc. 103 (1981) 5021–5023.
- [12] J. Augustynski, Chimia 42 (1988) 172–175.
- [13] W.M. Ayers, Spec. Publ. R. Soc. Chem. (1994) 365–374.
- [14] M. Azuma, K. Hashimoto, M. Hiramoto, M. Watanabe, T. Sakata, J. Electrochem. Soc. 137 (1990) 1772–1778.
- [15] V.S. Bagotzky, N.V. Osetrova, Russ. J. Electrochem. 31 (1995) 409–425.
- [16] A. Bandi, J. Electrochem. Soc. 137 (1990) 2157–2160.
- [17] A. Bandi, H.M. Kuhne, J. Electrochem. Soc. 139 (1992) 1605–1610.
- [18] R.P.S. Chaplin, A.A. Wragg, J. Appl. Electrochem. 33 (2003) 1107–1123.
- [19] P. Friebe, P. Bogdanoff, N. AlonsoVante, H. Tributsch, J. Catal. 168 (1997) 374–385.
- [20] A. Gennaro, A.A. Isse, M.G. Severin, E. Vianello, I. Bhugun, J.M. Saveant, J. Chem. Soc. Faraday Trans. 92 (1996) 3963–3968.
- [21] F. Goodridge, K. Lister, V. Guruswamy, J. Electrochem. Soc. 125 (1978) C176–C176.
- [22] K. Hara, A. Kudo, T. Sakata, J. Electroanal. Chem. 391 (1995) 141–147.
- [23] Y. Hori, A. Murata, R. Takahashi, S. Suzuki, J. Chem. Soc. Chem. Commun. (1988) 17–19.
- [24] Y. Hori, H. Wakebe, T. Tsukamoto, O. Koga, Electrochim. Acta 39 (1994) 1833–1839.

Table 2

Formic acid faradaic efficiencies ( $f$ ) and current densities ( $j$ ) for SnGDL electrode at the potentials applied for the electrolysis.

Potential (V) vs. SHE	SnGDL	
	$f$ (%)	$j$ ( $\text{mA cm}^{-2}$ )
$-0.8$	0	1.3
$-1.0$	2	5.7
$-1.2$	45	12.4
$-1.4$	63	17.1
$-1.6$	70	27.3
$-1.8$	62	15.0
$-2.0$	54	11.0



- [25] K. Ito, *Denki Kagaku* 58 (1990) 984–989.
- [26] M. Jitaru, D.A. Lowy, M. Toma, B.C. Toma, L. Oniciu, *J. Appl. Electrochem.* 27 (1997) 875–889.
- [27] A. Kitani, H. Yamada, K. Sasaki, *Denki Kagaku* 46 (1978) 570–572.
- [28] T. Mizuno, K. Ohta, A. Sasaki, T. Akai, M. Hirano, A. Kawabe, *Energy Source* 17 (1995) 503–508.
- [29] H. Nagao, T. Mizukawa, K. Tanaka, *Inorg. Chem.* 33 (1994) 3415–3420.
- [30] Y. Nakato, S. Yano, T. Yamaguchi, H. Tsubomura, *Denki Kagaku* 59 (1991) 491–498.
- [31] H. Noda, S. Ikeda, Y. Oda, K. Ito, *Chem. Lett.* (1989) 289–292.
- [32] Y.B. Vassiliev, V.S. Bagotsky, N.V. Osetrova, O.A. Khazova, N.A. Mayorova, *J. Electroanal. Chem.* 189 (1985) 271–294.
- [33] Y.B. Vassiliev, V.S. Bagotsky, O.A. Khazova, N.A. Mayorova, *J. Electroanal. Chem.* 189 (1985) 295–309.
- [34] M. Azuma, K. Hashimoto, M. Watanabe, T. Sakata, *J. Electroanal. Chem.* 294 (1990) 299–303.
- [35] A.F. Cherashev, A.P. Khrushch, *Russ. J. Electrochem.* 33 (1997) 181–185.
- [36] A.J. Morris, R.T. McGibbon, A.B. Bocarsly, *ChemSusChem* 4 (2011) 191–196.
- [37] A.F. Cherashev, A.P. Khrushch, *Russ. J. Electrochem.* 34 (1998) 410–417.
- [38] N. Gupta, M. Gattrell, B. MacDougall, *J. Appl. Electrochem.* 36 (2006) 161–172.
- [39] B. Innocent, D. Pasquier, F. Ropital, F. Hahn, J.M. Léger, K.B. Kokoh, *Appl. Catal. B* 94 (2010) 219–224.
- [40] F. Koleli, T. Atilan, N. Palamut, A.M. Gizir, R. Aydin, C.H. Hamann, *J. Appl. Electrochem.* 33 (2003) 447–450.
- [41] *in: For a commercial demonstration of a formic acid reactor powered by solar energy by Det Norske Veritas see <http://www.carboncapturejournal.com/displaynews.php?NewsID=751>, (accessed 08/2012).*
- [42] X. Yu, P.G. Pickup, *J. Power Sources* 182 (2008) 124–132.
- [43] F.A. Viva, 2009. Ph.D. thesis, University of Southern California, Los Angeles, USA.
- [44] G.K.S. Prakash, P. Suresh, F.A. Viva, G.A. Olah, *J. Power Sources* 181 (2008) 79–84.
- [45] G. Laurency, M. Grasmann, *Energy Environ. Sci.* 5 (2012) 8171–8181.
- [46] M. Czaun, A. Goepfert, R. May, R. Haiges, G.K.S. Prakash, G.A. Olah, *ChemSusChem* 4 (2011) 1241–1248. 10.1002/cssc.201000446.
- [47] W. Paik, T.N. Andersen, H. Eyring, *Electrochim. Acta* 14 (1969) 1217–1232.
- [48] S.R. Narayanan, B. Haimes, J. Soler, T.I. Valdez, *J. Electrochem. Soc.* 158 (2011) A167–A173.
- [49] M.N. Mahmood, D. Masheder, C.J. Harty, *J. Appl. Electrochem.* 17 (1987) 1159–1170.
- [50] S.D. Kapusta, N. Hackerman, *Electrochim. Acta* 25 (1980) 1625–1639.
- [51] A. Zhou, D. He, N. Xie, Q. Xie, L. Nie, S. Yao, *Electrochim. Acta* 45 (2000) 3943–3950.
- [52] A.J. Bard, L.R. Faulkner, *Electrochemical Methods. Fundamentals and Applications*, first ed., J. Wiley & Sons, 1980.
- [53] K.W. Frese, in: B.P. Sullivan, K. Krist, H.E. Guard (Eds.), *Electrochemical and Electrocatalytic Reactions of Carbon Dioxide*, Elsevier, Amsterdam, 1993, pp. 145–213.
- [54] S. Kapusta, N. Hackerman, *J. Electrochem. Soc.* 130 (1983) 607–613.
- [55] Y. Hori, K. Kikuchi, S. Suzuki, *Chem. Lett.* (1985) 1695–1698.
- [56] F. Koleli, T. Yesilkaynak, D. Balun, *Fresen. Environ. Bull.* 12 (2003) 1202–1206.
- [57] H. Noda, S. Ikeda, Y. Oda, K. Imai, M. Maeda, K. Ito, *Bull. Chem. Soc. Jpn.* 63 (1990) 2459–2462.
- [58] B. Innocent, D. Liaigre, D. Pasquier, F. Ropital, J.M. Léger, K. Kokoh, *J. Appl. Electrochem.* 39 (2009) 227–232.
- [59] H. Li, C. Oloman, *J. Appl. Electrochem.* 35 (2005) 955–965.
- [60] R.L. Machunda, H. Ju, J. Lee, *Curr. Appl. Phys.* 11 (2011) 986–988.